

Advective accretion onto a non-spherical accretor: a new scenario of shock formation

Sudeb Ranjan Datta,^{1*} Prasun Dhang^{2,3}, Bhupendra Mishra⁴

¹*Dept. of Physics, Indian Institute of Science, Bangalore-560012, India*

²*Institute for Advanced Study, Tsinghua University, Beijing-100084, China*

³*Department of Astronomy, Tsinghua University, Beijing-100084, China*

⁴*JILA, University of Colorado and National Institute of Standards and Technology, 440 UCB, Boulder, CO 80309-0440, USA*

Accepted XXX. Received YYY; in original form ZZZ

ABSTRACT

Numerous studies on hydrodynamics of the Keplerian as well as the sub-Keplerian accretion disc around a compact object (e.g., white dwarf (WD), neutron star (NS), or a black hole (BH)) attempted to explain the observed UV, soft and hard X-ray spectra. Although, when the compact object (e.g., a WD or an NS) has a finite surface, its rapid rotation, the stellar magnetic field could cause deformation of the spherical symmetry. Earlier studies for Keplerian disc showed that a deviation from the spherical symmetry of the compact object could affect the observed light curve and spectra at high frequencies. Here, we have explored the effect of the non-spherical nature of a compact object on the hydrodynamics of an optically thin, geometrically thick sub-Keplerian advective flow. We find that due to non-spherical shape of the central accretor, there is a possibility to trigger Rankine-Hugoniot shock in the sub-Keplerian advective flow close to the accretor without considering any general relativistic effect or presence of the hard surface of the star. Our results are more relevant for accretion onto WD as hardly any general relativistic effect will come in the picture. We propose that some observational features e.g., efficiency of fitting the spectra with multi-temperature plasma, hotter component of the flow having higher luminosity and hard X-ray QPOs in the non-magnetic cataclysmic variables can be explained by the presence of shock in the sub-Keplerian advective flow.

Key words:

1 INTRODUCTION

The physics of accretion discs has remained an open area of research since last few decades. Despite great progress in our understanding, we still need better theoretical model to shed light on recent observations. Generally, there are three theoretical models of accretion discs: (i) geometrically thin and optically thick Keplerian disc (Shakura & Sunyaev 1973), (ii) geometrically thick and optically thin advective flows (Chakrabarti 1989; Narayan & Yi 1994) and (iii) geometrically and optically thick slim discs (Abramowicz et al. 1988). Various accreting sources often show variability in observed luminosity and could change the geometrical shape of accretion discs.

Presence of a geometrically thick and optically thin advective flow is essential to explain hard X-rays and soft γ -rays from accreting systems like neutron stars (NSs) and black holes (BHs) (Chakrabarti & Titarchuk 1995; Narayan

et al. 1998; Yuan et al. 2005). Due to the advective properties of thick flows, thermal energy generated due to viscous dissipation gets advected into central object before it can escape vertically from the disc surface. The advection of thermal energy in such geometrically thick hot flows plays an important role in stabilization against thermal instability. Flow remains hot, optically thin, geometrically thick and is able to give higher energy photons (Narayan & Yi 1994, 1995). On the other hand in a Keplerian, optically thick, geometrically thin Shakura-Sunyaev disc (SSD) (Shakura & Sunyaev 1973; Novikov & Thorne 1973; Pringle 1981), emission of multi-temperature blackbody radiation is sufficient to balance the viscous heating. The resultant emission is observed in soft X-rays and is of higher luminosity. To explain the observed spectra, two-component accretion flow is also invoked (Chakrabarti & Titarchuk 1995; Chakrabarti 1996).

Several observations show that like BH and NS systems, accreting non-magnetic white dwarf systems (cataclysmic variables; CVs) also produce hard X-rays, the origin of which might be connected to the presence of a radiatively ineffi-

* E-mail: sudebd@iisc.ac.in

cient advection dominated flow (ADAF; Balman et al. 2014; Godon et al. 2017; Luna et al. 2018). However, Pringle & Savonije (1979) proposed the possibility of emission of hard X-rays from non-magnetic CVs depending on effectiveness of shock in a Keplerian SSD. For a detail discussion on the presence of an ADAF in non-magnetic CVs see section 5.2.

One crucial difference between the advective flow around the NS or the BH and that onto a WD is that protons are unable to transfer their energy to electrons and two temperature plasma comes into the picture for the former case (Narayan & Yi 1995; Rajesh & Mukhopadhyay 2010); while for the latter, temperature of the protons and the electrons remains almost the same (Medvedev & Menou 2002; Frank et al. 2002). Therefore, radiatively inefficient advective flow in CVs can be treated as a single temperature fluid (Chakrabarti 1989; Narayan & Popham 1993; Popham & Narayan 1995; Chakrabarti 1996).

It is probable that presence of the stellar rotation, strong stellar magnetic field and continuous accretion can change the spherical shape of the central accretor (Ostriker & Bodenheimer 1968; Ostriker & Hartwick 1968; Shapiro & Teukolsky 1983; Komatsu et al. 1989; Haskell et al. 2008; Das & Mukhopadhyay 2015; Subramanian & Mukhopadhyay 2015). One first-order generalization of spherical shape is Maclaurin Spheroid (MS; Chandrasekhar 1969). Deviation from the spherical symmetry of accreting source leads to change in gravitational force exerted on a test particle orbiting very close to it and could alter the dynamics of the accretion flow. Despite such an effect of gravity, the gravitational potential of an MS remains Newtonian.

There are already few theoretical studies on orbits around an MS (Amsterdamski et al. 2002; Kluźniak & Rosińska 2013) and SSDs around an MS accretor (Mishra & Vaidya 2015). These studies showed the emergence of many new features in the accretion flow just because of the deformation of the shape of the compact object. In this paper, we study the inviscid advective flow around an NS and a WD considering the accretor to be an MS. However, it must be emphasized that our reported model in this article is primarily applicable to WD since general relativistic (GR) effects do not play a crucial role in accretion discs around such a compact object. The importance of our reported theory could also be realized to describe accretion flow around rapidly rotating NS but not very precisely without including all the GR effects. Therefore, in the rest of the article, we primarily focus on accretion discs around WD rather than NS.

Shock can not be realized in the sub-Keplerian advective flow around a spherical Newtonian accretor, unless the effect of the hard surface of the accretor (Dhang et al. 2016) or the GR correction in the gravitational potential (Chakrabarti 1989, 1996; Mukhopadhyay 2002) are considered. For accretion on to a WD, to the best of our knowledge, we are reporting for the first time that formation of a shock is possible in the appropriate parameter space due to the deformed shape of the accretor. We propose that presence of shock in an ADAF around the non-magnetic CVs can explain different features in the observables such as inadequacy of single temperature component to fit the spectra, hotter region of the flow having higher luminosity and hard X-ray QPOs.

The plan of the paper is as follows. In section 2, we

present the formalism we follow. We analyze the parameter space for advective accretion flow in section 3. In section 4, we present the hydrodynamics of flow around an NS as well as a WD. We discuss the possible connection of our work to observations in section 5. Finally we concluded in section 6.

2 A GENERAL VIEW OF THE FORMALISM

We use a standard approach (e.g. see Chakrabarti 1989; Mukhopadhyay 2003) to investigate the inviscid accretion flow around a compact star (e.g. a neutron star or a white dwarf) whose gravity can be described by the gravitational force due to an MS. Specifically, we want to study the effects of deformation (may be due to rotation of the star or due to the intrinsic stellar magnetic field).

To obtain the flow variables, we solve conservation of mass (mass continuity equation) and momentum (radial momentum balance equation) as given below-

$$\frac{d}{dr}(r\Sigma v) = 0, \quad (1)$$

$$v \frac{dv}{dr} + \frac{1}{\rho} \frac{dP}{dr} - \frac{l^2}{r^3} + F(r) = 0, \quad (2)$$

where $\Sigma = 2\rho(r)h(r)$ is the vertically integrated surface density and $F(r)$ is the gravitational force for MS. Here, $\rho(r)$ is the density and $h(r)$ is the half-thickness of the disc. Unless otherwise stated, all the radial distances in this paper are in units of GM/c^2 , where M is the mass of the MS, G is the gravitational constant and c is the speed of light. The velocity v is in units of c and specific angular momentum l is in units of GM/c .

Along with equations (1) and (2), we use polytropic equation

$$P = K\rho^\gamma \quad (3)$$

to describe the equation of state. Where γ is the adiabatic index. Gravitational force due to MS at equatorial plane is

$$F(r) = \Omega^2 r = 2\pi G \rho_* (1 - e^2)^{1/2} e^{-3} (\gamma_r - \cos \gamma_r \sin \gamma_r) r \quad (4)$$

where e is the eccentricity and ρ_* is the density of MS, taken to be uniform. $\gamma_r = \sin^{-1}(ae/r)$, a is the semi-major axis of MS.

In dimensionless units, force takes the form

$$F(r) = 1.5(ae)^{-3} (\gamma_r - \cos \gamma_r \sin \gamma_r) r \quad (5)$$

and $h(r)$ can be found from the vertical equilibrium equation as

$$h(r) = c_s r^{1/2} F^{-1/2} \quad (6)$$

where $c_s = \sqrt{\gamma p / \rho}$ is the sound speed. Unless mentioned specifically, we use $\gamma=4/3$.

Now, combining equation (1) and (2) we get

$$\frac{dv}{dr} = \left[\frac{l^2}{r^3} - F(r) + \frac{c_s^2}{\gamma+1} \left(\frac{3}{r} - \frac{1}{F} \frac{dF}{dr} \right) \right] \bigg/ \left[v - \frac{2c_s^2}{(\gamma+1)v} \right] \quad (7)$$

Far away from the accretor, the radial velocity v is small and subsonic. As the flow approaches the accretor, v increases and in principle can exceed the local sound speed c_s

i.e. can become supersonic. This implies that at a critical radius r_c the denominator of equation (7) becomes zero i.e. at r_c , v becomes equal to $\sqrt{2/(\gamma+1)}c_s$. Though at $r = r_c$ $v \neq c_s$, due to historical reasons we use to say subsonic and supersonic flow before and after the critical point and we follow the same things in this work also. For a realistic flow, the presence of a non-divergent velocity gradient leads to the requirement that the numerator of equation (7) also vanishes so that we can use L'Hospital rule to have a definite $\left. \frac{dv}{dr} \right|_c$. Using L'Hospital's rule, the slope for velocity at critical point becomes

$$\left. \frac{dv}{dr} \right|_c = -\frac{B + \sqrt{B^2 - 4AC}}{2A} \quad (8)$$

where

$$A = 1 + \frac{2c_{sc}^2}{(\gamma+1)v_c^2} \left[1 + 2 \left(\frac{\gamma-1}{\gamma+1} \right) \right], \quad (9)$$

$$B = \frac{4c_{sc}^2(\gamma-1)}{v_c(\gamma+1)^2} \left(\frac{3}{r_c} - \frac{1}{F_c} \frac{dF}{dr} \right)_c, \quad (10)$$

$$C = \frac{3l^2}{r_c^4} + \left. \frac{dF}{dr} \right|_c + \frac{c_{sc}^2(\gamma-1)}{(\gamma+1)^2} \left[\frac{3}{r_c} + \frac{1}{F_c} \frac{dF}{dr} \right]_c^2 - \frac{c_{sc}^2}{\gamma+1} \left[\left(\frac{1}{F_c} \frac{dF}{dr} \right)_c^2 - \frac{1}{F_c} \frac{d^2F}{dr^2} \right]_c - \frac{3}{r_c^2} \quad (11)$$

Equating denominator and numerator of (7) to zero, we get Mach number

$$\mathcal{M}_c = \frac{v_c}{c_{sc}} = \sqrt{\frac{2}{\gamma+1}} \quad (12)$$

and sound speed

$$c_{sc} = \sqrt{(\gamma+1) \left(F_c - \frac{l^2}{r_c^3} \right) / \left(\frac{3}{r_c} - \frac{1}{F_c} \frac{dF}{dr} \right)_c} \quad (13)$$

at the critical point r_c . Now integrating equations 1 and 2, we can write down the energy and entropy of the flow at critical point as

$$E_c = \frac{2\gamma}{(\gamma-1)} \left[\left(F_c - \frac{l^2}{r_c^3} \right) / \left(\frac{3}{r_c} - \frac{1}{F_c} \frac{dF}{dr} \right)_c \right] + V_c + \frac{l^2}{2r_c^2} \quad (14)$$

and

$$\begin{aligned} \dot{\mu}_c &= (\gamma K)^n \dot{M} = r_c^{3/2} F_c^{-1/2} (\gamma+1)^{q/2} \\ &\times \left[\left(F_c - \frac{l^2}{r_c^3} \right) / \left(\frac{3}{r_c} - \frac{1}{F_c} \frac{dF}{dr} \right)_c \right]^{\gamma/(\gamma-1)} \end{aligned} \quad (15)$$

where $V_c = (\int F dr)|_c$, $q = (\gamma+1)/[2(\gamma-1)]$ and $n = 1/(\gamma-1)$. Here $\dot{\mu}$ carries the information of entropy. For non-dissipative system E remains constant throughout the flow. Here an important point to note is that formation of a shock enhances the entropy which changes the value of 'K'

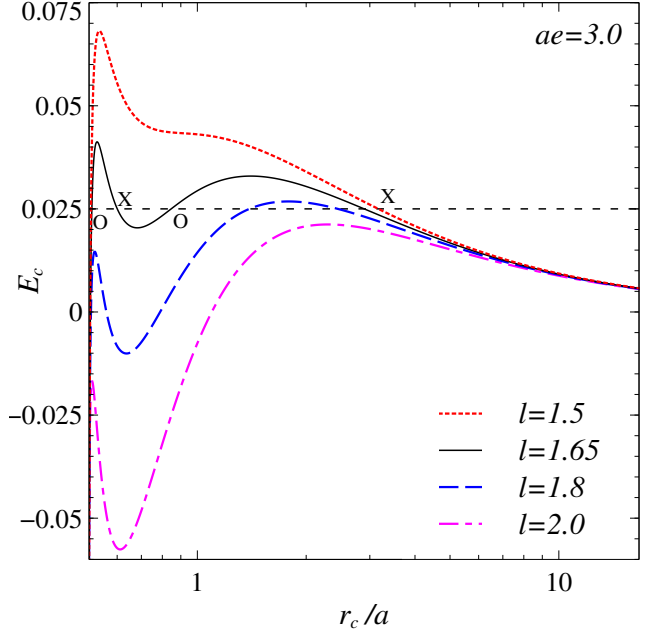


Figure 1. Variation of energy as a function of critical point location for various values of specific angular momentum (l). ae is fixed at 3.0. The horizontal line indicates constant energy of 0.025. Adiabatic index $\gamma=4/3$. Different types of critical points are marked in the figure. The x-axis values are presenting critical point location in terms of semi-major axis (a) of the compact object where a is assumed to be 6.0.

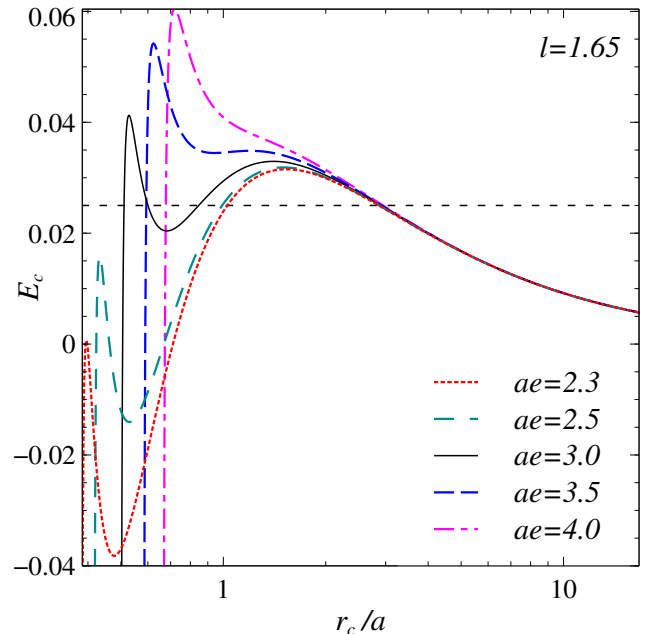


Figure 2. Variation of energy as a function of critical point location for different values of (semi-major axis(a) \times eccentricity(e)). l is fixed at 1.65. The horizontal line indicates constant energy of 0.025. Adiabatic index $\gamma=4/3$. The x-axis values are presenting critical point location in terms of semi-major axis (a) of the compact object where a is assumed to be 6.0. Keep in mind that only whole value of $a \times e$ affects the dynamics as well as energy.

which finally changes the value of $\dot{\mu}_c$. Therefore, \dot{M} remains same, while formation of a shock increases the value of $\dot{\mu}_c$.

Fig. 1 and 2 show the variation of energy at critical point (E_c) with position of critical point (r_c) for different l and ae values respectively. As we investigated here non-dissipative flow, so, fixing energy at critical point will fix the energy of the flow. Horizontal line in the Fig. 1 and 2 indicates the constant energy of the flow. It is clear that depending on E_c , critical points' locations as well as number of critical points also varies.

This opens up another possibility of formation of Rankine-Hugoniot shock (Landau 1987) in the flow. If we generalize the conditions to form a shock in accretion disc given by Chakrabarti (1989) for any compact object, we get

$$\frac{1}{2}\mathcal{M}_+^2 c_{s,sh+}^2 + nc_{s,sh+}^2 = \frac{1}{2}\mathcal{M}_-^2 c_{s,sh-}^2 + nc_{s,sh-}^2 \quad (16)$$

$$\frac{c_{sh+}^\nu}{\dot{\mu}_+} \left(\frac{2\gamma}{3\gamma-1} + \gamma\mathcal{M}_+^2 \right) = \frac{c_{sh-}^\nu}{\dot{\mu}_-} \left(\frac{2\gamma}{3\gamma-1} + \gamma\mathcal{M}_-^2 \right) \quad (17)$$

$$\dot{\mu}_+ > \dot{\mu}_- \quad (18)$$

where

$$\dot{\mu} = \mathcal{M}c_s^{2(n+1)} \frac{r_s^{3/2}}{\sqrt{F(r_s)}} \quad (19)$$

Here, the subscript 'sh' indicates the shock, '-' and '+' subscripts indicate before and after the shock. \mathcal{M} denotes the Mach number of the fluid and $\nu=(3\gamma-1)/(\gamma-1)$. Equation (18) indicates the natural choice of formation of shock as entropy increases after the shock. Combining equations (17) and (19), we get the shock invariant quantity as

$$SIQ = \frac{[2/\mathcal{M}_+ + (3\gamma-1)\mathcal{M}_+]^2}{\mathcal{M}_+^2(\gamma-1)+2} = \frac{[2/\mathcal{M}_- + (3\gamma-1)\mathcal{M}_-]^2}{\mathcal{M}_-^2(\gamma-1)+2} \quad (20)$$

If conditions (16), (18) and (20) are satisfied simultaneously by the flow, then shock will form in accretion disc.

3 ANALYSIS OF PARAMETER SPACE

In this section, we discuss the dependence of flow properties on different parameters such as eccentricity (e), radius of the central accretor (a), and specific angular momentum of the flow (l). Fig. 1 shows how the variation of specific angular momentum of the flow changes the number as well as location of critical points (Chakrabarti 1989) for fixed values of energy E_c and ae . For example, if we fix $ae=3.0$ as well as the energy of the flow at 0.025 then for $l = 1.65$, there are four critical points (where horizontal line of value 0.025 cuts E_c vs. r_c curves). The outer most critical point is a 'X' type critical point (Slope of E_c vs r_c curve is -ve). As we move inside, next critical points are 'O' type, 'X' type and 'O' type respectively. Chakrabarti (1990) discusses critical points and their types in detail. For the present purpose it is sufficient to state that 'X' type critical points are responsible for successful accretion. So, our current interest lies in the outer and inner 'X' type critical points. Hereafter

we indicate these two 'X' type critical points as outer and inner critical points. It is clear from Fig. 1 that for a definite range of specific angular momentum l , outer and inner critical points are present for a particular value of E_c and ae . While for a small angular momentum, the flow is more Bondi-like (Bondi 1952), for the flow with a sufficiently large angular momentum the centrifugal barrier opposes the accretion. It should be mentioned that the presence of both outer and inner critical points enhances the probability of shock in the flow (Chakrabarti 1989).

Next, we show how the change in eccentricity and radius affects critical point analysis. Treating central accretor as MS, fundamental difference is coming through the gravitational force it is applying on the test particle (Equation (5)) instead of spherical accretor. As this force does not involve a and e separately, change of the product of a and e only affects the results, not their individual values. Fig. 2 shows the E_c vs. r_c plots for different values of ae and a fixed l .

Equation (5) indicates that for a realistic $F(r)$, $r \geq ae$. Therefore, while doing a parameter space survey, we restrict to the limit $r \geq ae$ value. However, when we present the hydrodynamics of the accretion flow in the next section, we assume that disc truncates at the surface of the star of radius a . It may arise that the inner critical point lies inside a . In that case, we do the hydrodynamics considering the inner critical point and truncate the accretion flow at a to mimic the presence of a surface.

For a transonic flow around an accretor with a hard surface, shock in the accretion flow is almost inevitable because flow has to slow down at the surface (Dhang et al. 2016, 2018). Possibility of formation of the shock enhances in an inviscid sub-Keplerian transonic flow if both the outer and inner critical points coexist (Chakrabarti 1989, 1996; Mukhopadhyay 2003). In this work, we do not consider the effects of presence of the surface and assume there is a sink of mass at the inner boundary. To investigate the formation of shock in principle, we can solve the hydrodynamics from inner critical point and from outer critical point and can check whether the shock conditions (equations (16)-(20)) are satisfied or not in the region between two critical points. However, we follow in a more convenient way to check the possibility of shock which is by plotting E_c vs. $\dot{\mu}_c$ by varying r_c as shown in Fig. 3. This is usually called 'swallow-tail' picture (Fig. 3). For accretion with shock in the current context, the picture is like the following: matter from companion which is coming from far away reaches the outer critical point, becomes supersonic and then due to shock it jumps to the inner critical point branch and finally accretes by the compact object. In other scenarios, it may be possible to jump to other branches or shock may not happen and matter directly accretes to the compact object. For the present purpose we restrict ourselves to the scenario to jump to inner critical branch due to the formation of shock.

'Swallow-tail' picture gives the possible range of energy for which shock may form. In Fig. 3, 'O' and 'I' represent the branch for outer and inner critical point respectively. We need to find energy value for which matter can jump from the outer critical branch to inner critical branch with the necessary condition of increment of entropy as given in equation (18). The region ABD represents the possible region for the formation of shock. If we draw a constant

energy line (which is the energy of the flow) in this region, then matter may jump from low entropy region to high entropy region keeping its energy constant. Taking the energy value from this region, we need to check whether other conditions of the shock are satisfying or not. This ABD region merely gives only the possibility of shock. Increment of this region indicates the increment of the possibility of shock.

In Fig. 3 it is shown that how eccentricity of the MS changing the possibility of shock. We found that with decreasing eccentricity, the ABD region increases which indicates that decreasing eccentricity increases the possibility of formation of shock. However, for $e=0.4$ the curve from inner branch turns back and does not intersect with the outer branch. This returning nature is coming due to the presence of ‘O’ type critical point in the innermost region as described earlier. In the rest of the swallow-tail diagrams also, the curve turns back from the inner branch after some value. To keep the picture easy to understand, we have plotted up to that point beyond which returning occurs. For $e=0.4$ and lower values, there is no possible energy value which can intersect outer as well as inner branch with other specific parameters’ value. This denotes that for $e=0.4$ and beyond with fixed values of other parameters, inner and outer critical points cannot exist simultaneously. According to the present scenario of shock formation, shock will not form. From this analysis we can say that decreasing eccentricity of MS increases the probability of shock till the simultaneous occurrence of outer and inner critical points is possible.

4 HYDRODYNAMICS AROUND COMPACT OBJECT

In this section, we investigate the accretion structure around the two different kinds of compact objects namely NSs and WDs whose shape can be described by the MS. However, it should be mentioned that while the used Newtonian approach can explain the accretion flow around a WD, general relativistic effects are significant to consider in case of accretion disc around NS.

4.1 Around an NS

Here we describe the hydrodynamics of the accretion flow assuming the neutron star as an MS with typical observed values of mass $1M_{\odot}$, $a=6.0$. We have shown three cases depending on different realistic values of eccentricity (e) of NS and specific angular momentum (l) of the flow. In perfect combination of e and l , shock forms, but in other cases it disappears.

In section 3, we see that shock can form for a specific range of parameter space (l, e). A convenient way to check whether shock forms or not is to check the equality in equation (20). To study it, we simultaneously plot SIQ for two branches: when accretion happens through inner critical point and through outer critical point. Points of intersection give the locations of shock where flow jumps from outer critical branch to inner critical branch. This is shown in Fig. 4 for $l=1.65$ and $e=0.5$ when the E_c of the flow is 0.0289. Out of two possible shock locations, inner

one is unstable under radial perturbation due to post-shock acceleration. The outer one is stable due to post-shock deceleration (Nakayama 1992; Nobuta & Hanawa (1994)). So, the outer intersection point (B) is our desirable shock location. However, even the outer shock location is unstable to non-radial, non-axisymmetric perturbation (Iwakami et al. 2009). These instabilities (oscillations) are invoked to explain different time variabilities in the accreting systems (Molteni et al. 1996, 1999).

We consider both shocked and shock-free solutions. This is achieved by solving the equations for $\frac{dv}{dr}$ and $\frac{dc_s}{dr}$ simultaneously for different sets of l and e and keeping $E_c=0.0289$ fixed. We specify flow parameters at the critical points (where quantities are well determined, see section 2), and look for the stationary solutions.

Fig. 5 shows the radial profiles of the Mach number ($\mathcal{M}=v/c_s$) and sound speed (c_s) for the accretion flow around NS for $E_c=0.0289$, $a=6.0$ for three different sets of parameters: $l=1.65, e=0.5$; $l=1.5, e=0.5$; $l=1.65, e=0.55$. Although fixing E_c value to 0.0289 gives inner and outer critical point for set ($l=1.65, e=0.5$) only. However, same energy value gives only outer critical point for ($l=1.5, e=0.5$) and ($l=1.65, e=0.55$) which does not allow the formation of a shock. Therefore, only ($l=1.65, e=0.5$) gives us shock in advective flow among the three sets. It indicates that accreting matter of the same energy may or may not form shock depending on its specific angular momentum and eccentricity of the central accretor. At the shock, there is a sudden jump in Mach number as well as in sound speed, whereas there is a smooth increase in \mathcal{M} and c_s for other cases as gradually accreted by neutron star. Fig. 5 is extended till the inner critical point for shock solution. The vertical dotted line indicates the location of the surface where the flow will stop.

The beauty of the MS potential is in formation of the shock without incorporating any kind of general relativistic effect. Simultaneous formation of outer as well as inner critical points allows the formation of shock which is not possible using Newtonian potential of a spherical body. It should also be mentioned that the formation of shock in MS potential is possible even at lower l values compared to what is expected when Paczyński & Wiita (1980) pseudo-Newtonian potential is used for the same E_c .

4.2 Around a WD

Here we describe the hydrodynamics of the accretion flow around a WD which is assumed to be an MS with typical observed values of mass $0.6M_{\odot}$ with radius $0.013R_{\odot}$ (Parsons et al. (2017)). Conversion of this radius in unit of GM/c^2 gives $a \sim 10170$. Here we have assumed the eccentricity of the WD is 0.6. Godon et al. (2017) suggested for the presence of advective disc with radial size \sim white dwarf radius, which also varies from source to source. As these parameters’ values are suitable to form outer as well as inner critical point simultaneously, it opens up a new possibility of formation of shock within the flow for white dwarf accretion as presence of two critical points together is a necessary condition for shock formation!! Though it is not conventional, we used dimensionless unit to present length scales of white dwarf.

Here we have followed the same procedure as like for NS. Due to the larger size of WD, l also increases largely as Kep-

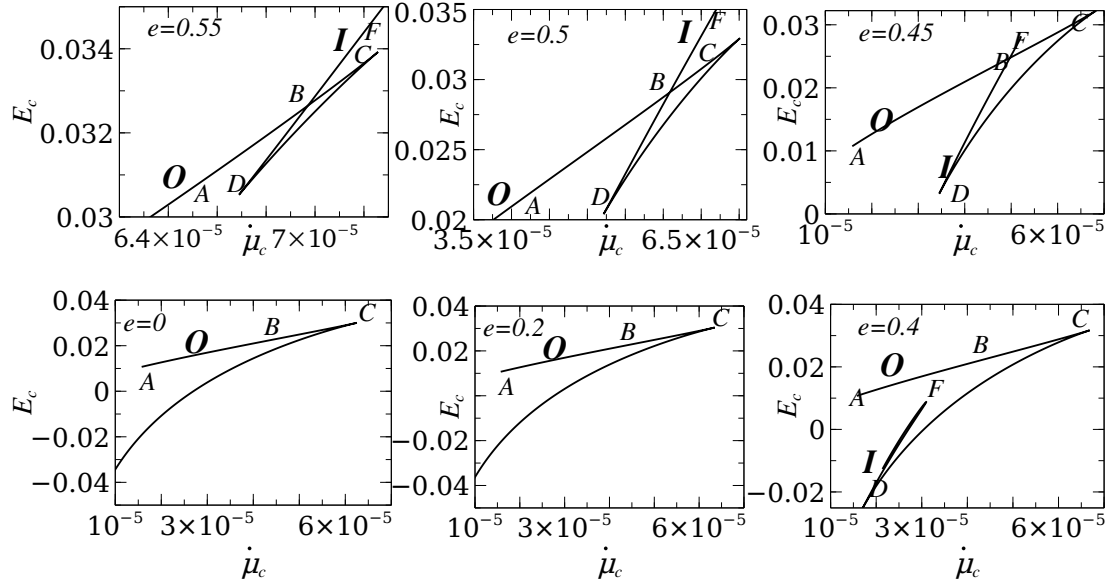


Figure 3. Variation of possibility of shock with different eccentricity. $a=6.0$ and $l=1.65$ is fixed for all the figures. **O** and **I** are representing outer and inner critical branch respectively. ABD area is giving the energy range in which both branch exist simultaneously and shock can occur. It shows that decreasing e increases the possibility of shock up to a certain value for which shock can occur i.e. till when two branches exist simultaneously.

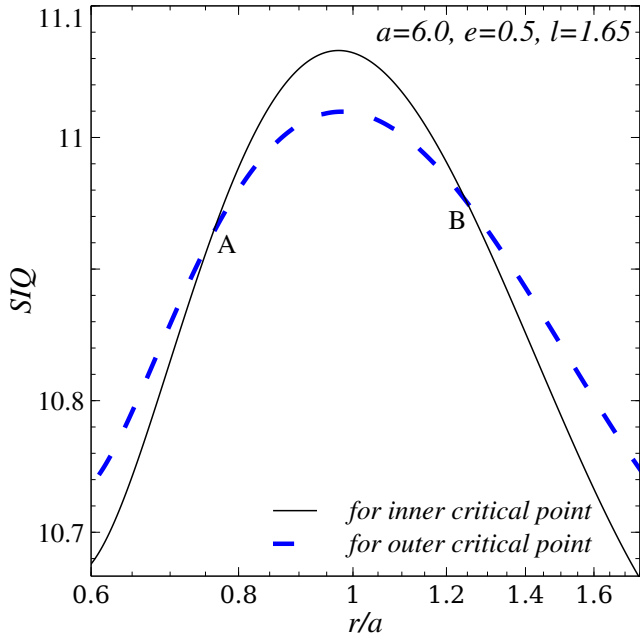


Figure 4. Variation of shock invariant quantity with radial distance for accretion flow with $E_c=0.0289$ and $l=1.65$ around neutron star. Two curves are for accretion through outer and inner critical point. The intersection points (A and B) of the two curves indicate the possible shock locations where inner one (A) is unstable and outer one (B) is representing the actual location of shock

lerian angular momentum is proportional to \sqrt{r} . For advective flow with $E_c=1.76e-5$, $l=71.0$ around WD with $e=0.6$, there is simultaneous occurrence of outer as well as inner critical point. In Fig. 6, we have overplotted the SIQ for two

cases when accretion happens through outer as well as inner critical point. The outer intersection point (B) gives our desired shock location. We have shown radial profiles for \mathcal{M} and c_s for $E_c=1.76e-5$ for three different sets: $l=71.0$, $e=0.6$; $l=70.2$, $e=0.6$; $l=71.0$, $e=0.7$ in Fig. 7. Only for ($l=71.0$, $e=0.6$) shock occurs, and there is a steep increase in c_s and a decrease in \mathcal{M} . For other two sets, shock disappears and there is gradual increase of \mathcal{M} and c_s as matter goes inward through accretion. It indicates again that for certain parameters' range only shock can occur. For a specific value of E_c , only certain range of l and ae values will result in shock. Fig. 7 is extended till the inner critical point for shock solution. The vertical dotted line indicates the location of the surface where the flow will stop.

Here the result is more robust as hardly any general relativistic effect will come in the picture and also formation of shock is not possible within accretion flow in Newtonian potential of a spherical body. So, wholly new phenomena arise only due to deformation of the shape of the accreting white dwarf. To the best of our knowledge we suppose, for the first time we are reporting this kind of shock formation for white dwarf accretion. As the formation of accretion disc is possible only for non-magnetic CVs, only spinning of WD should be sufficient to deform it. This is justified in discussion section further from observational point of view.

5 DISCUSSION

We have discussed the hydrodynamics around an NS, as well as around a WD. However, we must emphasize that the Newtonian description of the hydrodynamics is more suitable to describe the accretion physics around a WD compared to that around an NS; where general relativistic effects are important. Our proposed model is specifically applicable to the non-magnetic Cataclysmic Variables (CVs) where stel-

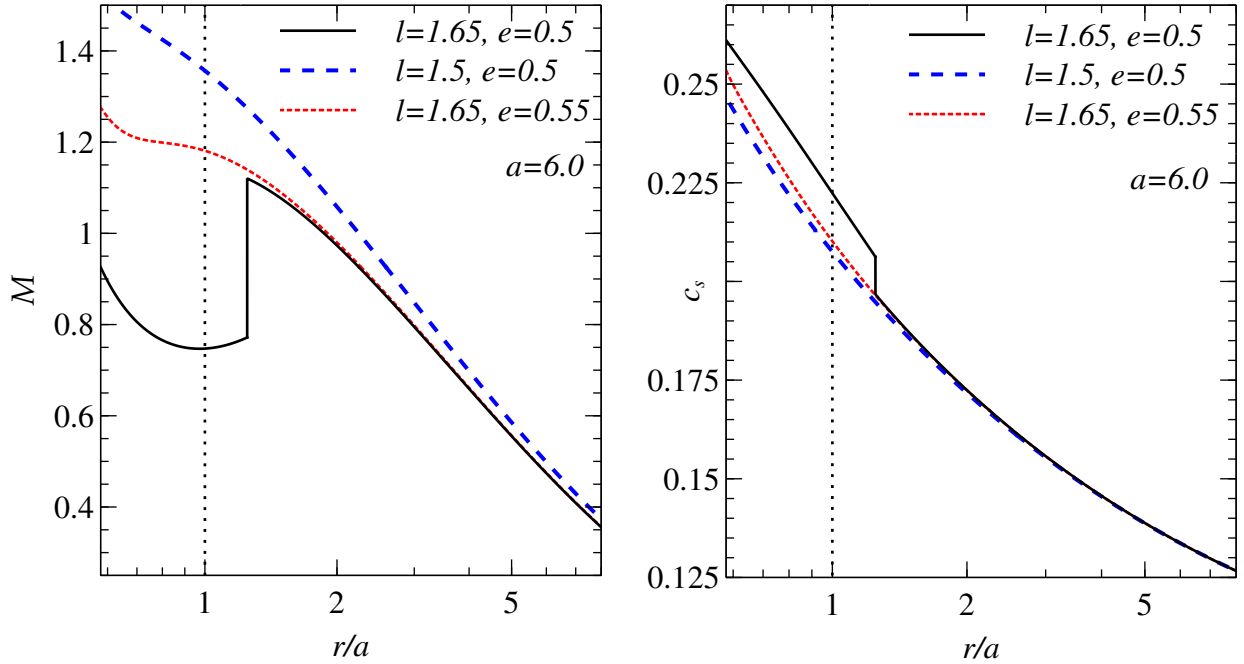


Figure 5. Variation of Mach number (\mathcal{M}) and sound speed (c_s) with radius with and without formation of shock for different combination of l and e . The x-axis is presenting radius in terms of a . Combination of $l=1.65$ and $e=0.5$ gives $r_{c,in}/a=0.58$ and $r_{c,out}/a=2.24$ for $E_c=0.0289$ which makes shock possible at $r_{sh}/a=1.25$. The plot is extended till inner critical point for shock solution. The vertical dotted line at $r/a=1$ indicates the surface of the neutron star.

lar magnetic field has a non-negligible effect on the accretion, unlike polars or intermediate polars (for a review see Mukai 2017). Observations reveal, more than 70% of the WDs have magnetic field strength less than 10K Gauss (Aznar Cuadrado et al. 2004; Valyavin et al. 2006; Scaringi et al. 2017; Patterson 1994).

The non-magnetic CVs are broadly classified into the novalikes (NLs) and dwarf novae (DNe). NLs spend most of their time in a high state (i.e high mass accretion rate) with UV emission predominantly originating from the disc (La Dous 1991); while DNe are observed mostly in the quiescent state (low mass accretion rate) (Hack et al. 1993). However, DNe show periodic outbursts (high mass accretion rate) with disc dominated UV.

5.1 Is sufficient deformation of WD possible?

Before drawing any connection of the described model with the observed phenomena in non-magnetic CVs, we would like to check the justification of the considered stellar deformation quantified by the parameter e . Within the limited observed samples it has been estimated that the spin frequency Ω_* of many non-magnetic CVs lies in the range $0.2 - 0.3 \Omega_K$ (Sion 1999; Godon et al. 2012), where Ω_K is the Keplerian angular velocity at the surface of the WD. However, Pandel et al. (2005) suggested that the upper limit of rotational velocity of WD (i.e. rotational velocity of boundary layer) lies within range of $(0.2 - 0.4) \Omega_K$. Such values of Ω_* are good enough to generate the eccentricity e (≈ 0.6) (equation

(7.3.18) of Shapiro & Teukolsky 1983, Chandrasekhar 1969) of the WD considered in our work.

5.2 Advective flows in CVs

The UV spectra from the disc-dominated non-magnetic CVs are generally modeled using the standard disc model (Wade & Hubeny 1998). However, a significant fraction of the theoretical spectra were found to be too blue compared to the observed UV spectra (Linnell et al. 2005; Puebla et al. 2007; Godon et al. 2017).

Because of the presence of the hard surface in the WD, a boundary layer (BL) is expected to form between the stellar surface and the Keplerian disc (Pringle 1981; Frank et al. 2002). BL is predicted to be optically thick and to emit soft X-rays during high accretion states (high states in NLs and outbursts in DNe) (Narayan & Popham 1993; Popham & Narayan 1995), while hard X-ray is expected from an optically thin BL region during quiescence (Pringle & Savonije 1979; Narayan & Popham 1993). Although hard X-ray is observed in quiescent sources as expected (Szkody et al. 2002; Pandel et al. 2005), many sources very often exhibit optically thin hard X-ray emission in the high accretion states (van Teeseling et al. 1996; Balman et al. 2014).

Inadequacy of the standard disc model in explaining observed UV spectra in high states (Godon et al. 2017) and presence of the optically thin hard X-ray in low as well as in high accretion states (Balman & Revnivtsev 2012) lead to the possibility that the radiatively inefficient hot advective

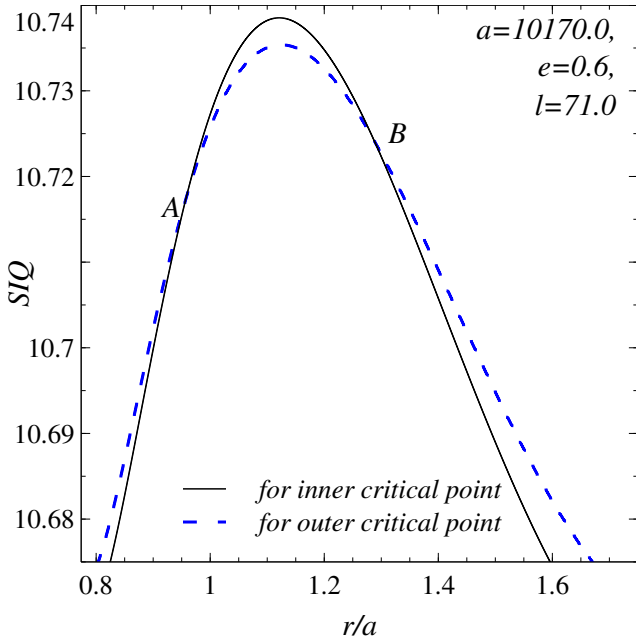


Figure 6. Variation of shock invariant quantity with radial distance for accretion flow with $E_c=1.76e-5$ and $l=1.65$ around white dwarf. Two curves are for accretion through outer and inner critical point. The intersection points (A and B) of the two curves indicate the possible shock locations where inner one (A) is unstable and outer one (B) is representing the actual location of shock

accretion flows (ADAF-like) exist in non-magnetic CVs. It is thought that an outer optically thick Keplerian disc is truncated to optically thin hot advective flow in the quiescent DNe (for reviews see Lasota 2001, 2004). The outer Keplerian disc moves inward as mass accretion rate increases during the outbursts (Balman & Revnivtsev 2012). Recent observations suggest that NLs too have a truncated disc with optically thin BLs merged with a hot advective flow (Balman et al. 2014; Godon et al. 2017). Therefore a natural expectation is that a hot advective flow is supposed to exist both in low and in high accretion states of non-magnetic CVs.

5.3 Connection of shock in advective flows to spectra and time variabilities

Presence of the shock in the hot radiatively inefficient advective accretion flow around the deformed WD leads to certain features which can explain different observables in non-magnetic CVs. We shall discuss the plausible connections among the observables and shocked flow one by one.

5.3.1 Spectra

The spectra from accreting WDs used to be modeled as multi-temperature isobaric cooling flow (power law and/or Bremsstrahlung) (mkcflow/CEVMKL in XSPEC or using two/more MEKAL components) (Mukai 2017 and references therein). In this model, the emission measure at each temperature is proportional to the time the cooling gas remains

at that temperature. For most of the accreting WDs, multi-MEKAL component significantly improves the spectra in comparison with single component (Mauche & Mukai 2002; Pandel et al. 2005; Balman & Revnivtsev 2012). To match the full spectra accurately, blackbody (originated from Keplerian disc part) used to be added along with the above optically thin emission.

One of the characteristic property of advective flows is that the inward flow velocity increases very rapidly as it approaches the central accretor (Chakrabarti 1989; Narayan & Yi 1994; Chakrabarti 1996). The rapid increase in radial velocity also seen in the shock-free solutions denoted by the short and long dashed curves in Figs. 5 and 7. Large radial velocity close to the accretor gives very little time to the flow for emission. Therefore, it will be hard to distinguish the regions with different temperatures within the same flow as the emission measure at a temperature depends on the time the flow spends at that temperature. Occurrence of shock in the advective flow (as discussed in sections 3 and 4.2) leads to the rise in temperature ($\sim c_s^2$) as well as an increase in density in the post-shock region. In addition, in the post-shock flow, the radial velocity decreases substantially, leading to a longer time span of the flow at higher temperatures. Therefore, it is expected to have higher emission from hotter and denser post-shock region compared to unshocked flow and this may make the regions with different temperatures more distinguishable in the whole spectra.

Hence, we see that the presence of a shock in the optically thin sub-Keplerian flow close to the accretor has the potential to explain the following features: inadequacy of single MEKAL component and efficiency of multi-component MEKAL to fit the spectra of non-magnetic CVs, higher luminosity of the hotter component of the accretion flow (as observed in case of Mv Lyr; Balman et al. 2014).

5.3.2 Time variabilities

CVs show a wide range of time variabilities. The rapid variabilities are seen in optical, UV as well as in X-ray bands with time scales ranging from \sim second to \sim kilo seconds (for a review, see Warner 2004). The diverse nature of the variabilities leads to the possibility that they are of different origin. In general in magnetic CVs (polars and intermediate polars) time variabilities are associated with the magnetically channelled accretion. The optical dwarf nova oscillations (DNOs) are modeled to be due to the magnetic coupling in an equatorial belt (Paczynski & Zytkow 1978; Warner & Woudt 2002), while the quasi periodic oscillations (QPOs) are said to be generated by the magnetically excited traveling waves in the disc (Warner & Woudt 2002). It is also suggested that QPOs are the oscillations of the intrinsic luminosity of the disc itself (Carroll et al. 1985; Collins et al. 2000). However, the hard X-ray QPOs (with time-scales $\sim 20 - 1000$ s) are said to have a different origin and are connected to the transition between optically thick and optically thin discs (Wheatley et al. 2003).

Presence of the shock in the advective flow in non-magnetic CVs lead to an exciting possibility of explaining the underlying mechanism generating QPOs seen in hard X-rays. This is because the standing shock becomes unstable (oscillatory) under non-radial non-axisymmetric perturbations (Foglizzo 2002; Blondin et al. 2003; Iwakami et al.

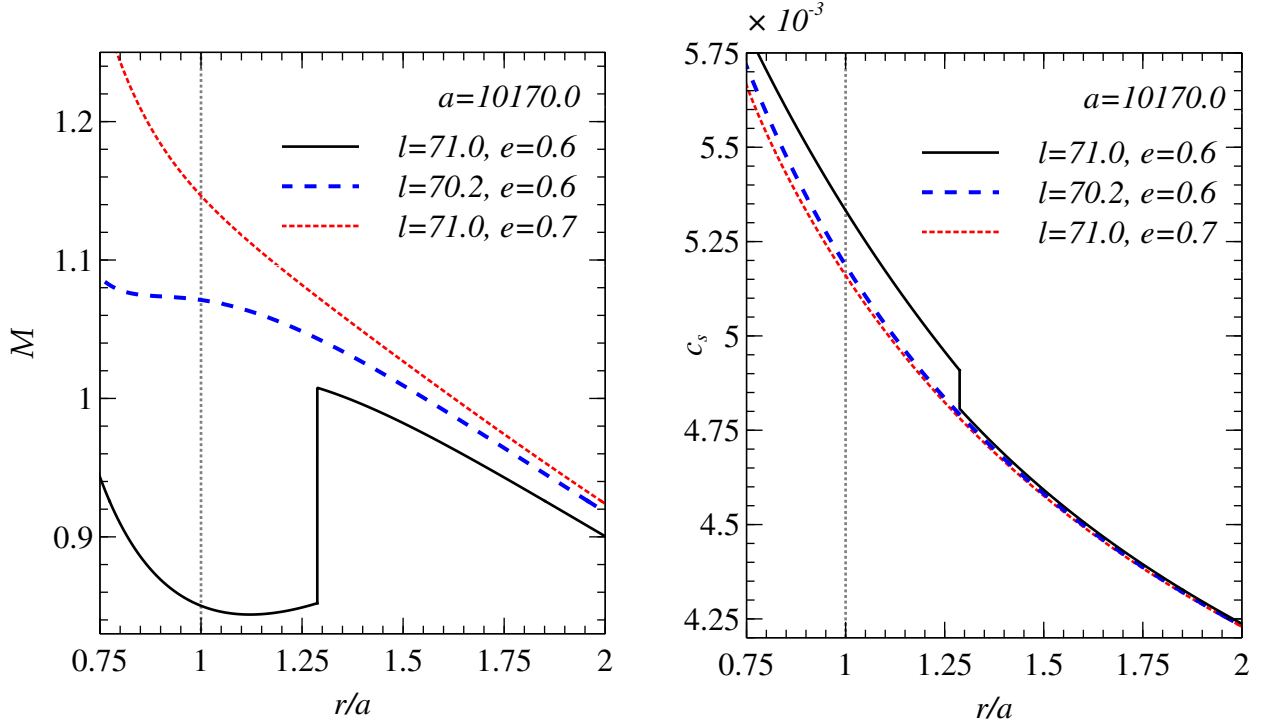


Figure 7. Variation of Mach number (\mathcal{M}) and sound speed (c_s) with radius same as Fig. 5 but here compact object is white dwarf. Here combination of $l=71.0$ and $e=0.6$ gives $r_{c,in}/a=0.77$ and $r_{c,out}/a=1.85$ (~ 0.00001 Astronomical units) for $E_c=1.76e-5$ which makes shock possible at $r_{sh}/a=1.29$. The plot is extended till inner critical point for shock solution. The vertical dotted line $r/a=1$ indicates the surface of the white dwarf.

2009; Dhang et al. 2016). Even in 1D, shock becomes unstable in the presence of cooling (Chevalier & Imamura 1982; Saxton 2002). The oscillation of the hot dense post-shock region in principle can generate modulation in the observed light curve (Molteni et al. 1996, 1999) with the time scale half the oscillation period T_{osc} , where

$$T_{osc} = \int_{r_{in}}^{r_{sh}} \left(\frac{dr}{|v_r|} + \frac{dr}{|c_s - v_r|} \right) \quad (21)$$

(for details see section 5.1.4 and 6.3 of Dhang et al. 2018). Study of rapid X-ray variability and its underlying mechanism is specially attractive in the context of the proposed ESA mission - Large Observatory for X-ray Timing (LOFT), which will have excellent timing as well as spectral resolution (Feroci et al. 2014; de Martino et al. 2015).

6 SUMMARY

In this paper, we have studied the hydrodynamics of an optically thin advective flow around a deformed (from spherical shape) compact object which has a finite surface e.g., an NS or a WD. We treat the deformed star as a Maclaurin Spheroid (MS). The key findings of the work are mentioned below.

- Treating compact object as an MS opens up a new possibility for formation of Rankine-Hugoniot shock which is not possible for accretion around a spherical accretor with-

out considering GR effects or effects of the hard surface of the accretor.

- To the best of our knowledge, for the first time we are reporting the possibility of occurrence of a shock in the radiatively inefficient hot advective flow around a WD. As far as we are concerned to understand the flow hydrodynamics around the non-magnetic CVs, our findings are robust as flow around a WD hardly deviates from the Newtonian regime.

- Shock impedes the gradual increase of flow velocity near the compact object. Density and temperature jump to higher values and velocity drops to a lower value in the post shock region. Hence a hotter, and larger emission is expected from the post-shock region compared to that from the preshock glow. We propose that the presence of a shock in the ADAF-like flows in the non-magnetic CVs can explain the efficiency of multi-component MEKAL to fit the spectra and a higher luminosity of the higher temperature component.

- The accretion shock becomes unstable (oscillatory) under the non-radial non-axisymmetric perturbations. The oscillation of the hot dense post-shock region can be the underlying mechanism behind the observed QPOs in hard X-ray.

ACKNOWLEDGEMENTS

We would like to thank Banibrata Mukhopadhyay, Vikram Rana and Tushar Mondal for their useful discussion. This

work is partly supported by the fund of DST INSPIRE fellowship belonging to SRD.

REFERENCES

- Abramowicz M. A., Czerny B., Lasota J. P., Szuszkiewicz E., 1988, *ApJ*, **332**, 646
- Amsterdamski P., Bulik T., Gondek-Rosińska D., Kluźniak W., 2002, *A&A*, **381**, L21
- Aznar Cuadrado R., Jordan S., Napiwotzki R., Schmid H. M., Solanki S. K., Mathys G., 2004, *A&A*, **423**, 1081
- Balman Ş., Revnivtsev M., 2012, *A&A*, **546**, A112
- Balman Ş., Godon P., Sion E. M., 2014, *ApJ*, **794**, 84
- Blondin J. M., Mezzacappa A., DeMarino C., 2003, *ApJ*, **584**, 971
- Bondi H., 1952, *MNRAS*, **112**, 195
- Carroll B. W., McDermott P. N., Savedoff M. P., van Horn H. M., Cabot W., 1985, *ApJ*, **296**, 529
- Chakrabarti S. K., 1989, *ApJ*, **347**, 365
- Chakrabarti S. K., 1990, Theory of Transonic Astrophysical Flows. World Scientific Publishing Co, doi:10.1142/1091
- Chakrabarti S. K., 1996, *ApJ*, **464**, 664
- Chakrabarti S., Titarchuk L. G., 1995, *ApJ*, **455**, 623
- Chandrasekhar S., 1969, Ellipsoidal figures of equilibrium
- Chevalier R. A., Imamura J. N., 1982, *ApJ*, **261**, 543
- Collins T. J. B., Helfer H. L., Van Horn H. M., 2000, *ApJ*, **534**, 934
- Das U., Mukhopadhyay B., 2015, *J. Cosmology Astropart. Phys.*, **2015**, 016
- Dhang P., Sharma P., Mukhopadhyay B., 2016, *MNRAS*, **461**, 2426
- Dhang P., Sharma P., Mukhopadhyay B., 2018, *MNRAS*, **476**, 3310
- Feroci M., et al., 2014, The Large Observatory for x-ray timing. p. 91442T, doi:10.1117/12.2055913
- Foglizzo T., 2002, *A&A*, **392**, 353
- Frank J., King A., Raine D. J., 2002, Accretion Power in Astrophysics: Third Edition
- Godon P., Sion E. M., Levay K., Linnell A. P., Szkody P., Barrett P. E., Hubeny I., Blair W. P., 2012, *ApJS*, **203**, 29
- Godon P., Sion E. M., Balman Ş., Blair W. P., 2017, *ApJ*, **846**, 52
- Hack M., Ladous C., Jordan S. D., Thomas R. N., Goldberg L., Pecker J.-C., 1993, Cataclysmic variables and related objects. Vol. 507
- Haskell B., Samuelsson L., Glampedakis K., Andersson N., 2008, *MNRAS*, **385**, 531
- Iwakami W., Kotake K., Ohnishi N., Yamada S., Sawada K., 2009, *ApJ*, **700**, 232
- Kluźniak W., Rosińska D., 2013, *MNRAS*, **434**, 2825
- Komatsu H., Eriguchi Y., Hachisu I., 1989, *MNRAS*, **237**, 355
- La Dous C., 1991, *A&A*, **252**, 100
- Landau L., 1987, Fluid Mechanics: Landau and Lifshitz Course of Theoretical Physics, vol. 6
- Lasota J.-P., 2001, *New Astron. Rev.*, **45**, 449
- Lasota J. P., 2004, in Tovmassian G., Sion E., eds, Revista Mexicana de Astronomia y Astrofisica Conference Series Vol. 20, Revista Mexicana de Astronomia y Astrofisica Conference Series. pp 124–127 (arXiv:astro-ph/0402190)
- Linnell A. P., Szkody P., Gänsicke B., Long K. S., Sion E. M., Hoard D. W., Hubeny I., 2005, *ApJ*, **624**, 923
- Luna G. J. M., et al., 2018, *A&A*, **616**, A53
- Mauche C. W., Mukai K., 2002, *ApJ*, **566**, L33
- Medvedev M. V., Menou K., 2002, *ApJ*, **565**, L39
- Mishra B., Vaidya B., 2015, *MNRAS*, **447**, 1154
- Molteni D., Sponholz H., Chakrabarti S. K., 1996, *ApJ*, **457**, 805
- Molteni D., Tóth G., Kuznetsov O. A., 1999, *ApJ*, **516**, 411
- Mukai K., 2017, *PASP*, **129**, 062001
- Mukhopadhyay B., 2002, *ApJ*, **581**, 427
- Mukhopadhyay B., 2003, *ApJ*, **586**, 1268
- Nakayama K., 1992, *MNRAS*, **259**, 259
- Narayan R., Popham R., 1993, *Nature*, **362**, 820
- Narayan R., Yi I., 1994, *ApJ*, **428**, L13
- Narayan R., Yi I., 1995, *ApJ*, **452**, 710
- Narayan R., Mahadevan R., Quataert E., 1998, in Abramowicz M. A., Björnsson G., Pringle J. E., eds, Theory of Black Hole Accretion Disks. pp 148–182 (arXiv:astro-ph/9803141)
- Nobuta K., Hanawa T., 1994, *PASJ*, **46**, 257
- Novikov I. D., Thorne K. S., 1973, in Dewitt C., Dewitt B. S., eds, Black Holes (Les Astres Occlus). pp 343–450
- Ostriker J. P., Bodenheimer P., 1968, *ApJ*, **151**, 1089
- Ostriker J. P., Hartwick F. D. A., 1968, *ApJ*, **153**, 797
- Paczynski B., Zytow A., 1978, in Second Symposium of Problem Comm. Physics and Evolution of Stars, Warsaw, Poland, June. pp 20–251977
- Paczyński B., Wiita P. J., 1980, *A&A*, **88**, 23
- Pandel D., Córdova F. A., Mason K. O., Priedhorsky W. C., 2005, *ApJ*, **626**, 396
- Parsons S. G., et al., 2017, *MNRAS*, **470**, 4473
- Patterson J., 1994, *PASP*, **106**, 209
- Popham R., Narayan R., 1995, *ApJ*, **442**, 337
- Pringle J. E., 1981, *ARA&A*, **19**, 137
- Pringle J. E., Savonije G. J., 1979, *MNRAS*, **187**, 777
- Puebla R. E., Diaz M. P., Hubeny I., 2007, *AJ*, **134**, 1923
- Rajesh S. R., Mukhopadhyay B., 2010, *MNRAS*, **402**, 961
- Saxton C. J., 2002, *Publ. Astron. Soc. Australia*, **19**, 282
- Scaringi S., Maccarone T. J., D’Angelo C., Knigge C., Groot P. J., 2017, *Nature*, **552**, 210
- Shakura N. I., Sunyaev R. A., 1973, *A&A*, **24**, 337
- Shapiro S. L., Teukolsky S. A., 1983, Black holes, white dwarfs, and neutron stars: The physics of compact objects
- Sion E. M., 1999, *PASP*, **111**, 532
- Subramanian S., Mukhopadhyay B., 2015, *MNRAS*, **454**, 752
- Szkody P., Nishikida K., Raymond J. C., Seth A., Hoard D. W., Long K. S., Sion E. M., 2002, *ApJ*, **574**, 942
- Valyavin G., Bagnulo S., Fabrika S., Reisenegger A., Wade G. A., Han I., Monin D., 2006, *ApJ*, **648**, 559
- Wade R. A., Hubeny I., 1998, *ApJ*, **509**, 350
- Warner B., 2004, 116, 115
- Warner B., Woudt P. A., 2002, *MNRAS*, **335**, 84
- Wheatley P. J., Mauche C. W., Mattei J. A., 2003, *MNRAS*, **345**, 49
- Yuan F., Cui W., Narayan R., 2005, *ApJ*, **620**, 905
- de Martino D., et al., 2015
- van Teeseling A., Beuermann K., Verbunt F., 1996, *A&A*, **315**, 467

This paper has been typeset from a $\text{\TeX}/\text{\LaTeX}$ file prepared by the author.